2015

Processable conducting graphene/chitosan hydrogels for tissue engineering

Sepidar Sayyar
University of Wollongong, sepidar@uow.edu.au

Eoin Murray
University of Wollongong, eoin@uow.edu.au

Brianna Thompson
University of Wollongong, brianna@uow.edu.au

Johnson Chung
Univeristy Of Wollongong, johnsonc@uow.edu.au

David L. Officer
University of Wollongong, davido@uow.edu.au

See next page for additional authors

Publication Details

Sayyar, S., Murray, E., Thompson, B. C., Chung, J., Officer, D. L., Gambhir, S., Spinks, G. M. & Wallace, G. G. (2015). Processable conducting graphene/chitosan hydrogels for tissue engineering. Journal of Materials Chemistry B, 3 (3), 481-490.

Processable conducting graphene/chitosan hydrogels for tissue engineering

Abstract
Composites of graphene in a chitosan-lactic acid matrix were prepared to create conductive hydrogels that are processable, exhibit tunable swelling properties and show excellent biocompatibility. The addition of graphene to the polymer matrix also resulted in significant improvements to the mechanical strength of the hydrogels, with the addition of just 3 wt% graphene resulting in tensile strengths increasing by over 200%. The composites could be easily processed into three-dimensional scaffolds with finely controlled dimensions using additive fabrication techniques and fibroblast cells demonstrate good adhesion and growth on their surfaces. These chitosan-graphene composites show great promise for use as conducting substrates for the growth of electro-responsive cells in tissue engineering.

Keywords
engineering, tissue, graphene, hydrogels, chitosan, conducting, processable

Disciplines
Engineering | Physical Sciences and Mathematics

Publication Details
Sayyar, S., Murray, E., Thompson, B. C., Chung, J., Officer, D. L., Gambhir, S., Spinks, G. M. & Wallace, G. G. (2015). Processable conducting graphene/chitosan hydrogels for tissue engineering. Journal of Materials Chemistry B, 3 (3), 481-490.

Authors
Sepidar Sayyar, Eoin Murray, Brianna Thompson, Johnson Chung, David L. Officer, Sanjeev Gambhir, Geoffrey M. Spinks, and Gordon G. Wallace

Cite this: DOI:

Processable Conducting Graphene/Chitosan Hydrogels for Tissue Engineering.

S. Sayyar,[a] E. Murray,[b*] B. C. Thompson,[c] J. Chung, D. L. Officer,[a] S. Gambhir,[a] G. M. Spinks[a,] and G. G. Wallace[a*]

Received
Accepted

DOI:

Composites of graphene in a chitosan-lactic acid matrix were prepared to create conductive hydrogels that are processable, exhibit tunable swelling properties and show excellent biocompatibility. The addition of graphene to the polymer matrix also resulted in significant improvements to the mechanical strength of the hydrogels, with the addition of just 3 wt% graphene resulting in tensile strengths increasing by over 200 %. The composites could be easily processed into three-dimensional scaffolds with finely controlled dimensions using additive fabrication techniques and fibroblast cells demonstrate good adhesion and growth on their surfaces. These chitosan-graphene composites show great promise for use as conducting substrates for the growth of electro-responsive cells in tissue engineering.

Introduction

Modern tissue engineering techniques seek to overcome the limitations of traditional medical procedures that require the repair or replacement of tissues. In these techniques, cells adhere to three-dimensional scaffolds, which provide structural support while the tissue regenerates to repair the damaged tissue and organs. One of the major limitations in tissue engineering is the development of suitable materials for these scaffolds. [1] The processability of the material, the correct physical properties and cellular compatibility are the major factors that determine the suitability of these materials. Traditional polymeric materials are commonly used for tissue scaffolds but lack some desirable properties [2], such as electrical conductivity that has been shown to be beneficial as electrical stimulation can improve the growth of electro-responsive cells such as nerve and muscle cells.[3-5] The introduction of an electrically conducting filler to a polymeric matrix can not only produce electrically conducting scaffolds, but can also improve the tensile strength.

Chitosan is a semi-crystalline natural polymer with good biocompatibility and biodegradability that has been used in a variety of applications such as artificial skin, tissue engineering and drug delivery.[6] Chitosan is a derivative of chitin and is obtained by the partial deacetylation of chitin under alkaline conditions or by enzymatic hydrolysis in the presence of a chitin deacetylase. However, poor mechanical properties restrict its application in certain fields. It has been shown that the incorporation of nanofillers and the synthesis of composites provide effective routes to improve the physico/chemical properties of such biopolymers.[7-10] Chitosan is an ideal polymer for composite synthesis as multiple functional groups on the chitosan backbone result in easy covalent or physisorbed attachment of filler materials to the polymer matrix.

Graphene is a single layer two-dimensional carbon material arranged in a honeycomb lattice. [11] This nanostructured material is regarded as an ideal reinforcing filler in the preparation of polymer

composites due to its high aspect ratio and excellent mechanical, electrical, optical, thermal and magnetic properties.[12, 13] In contrast to other widely used nanomaterial fillers such as carbon nanotubes, the synthesis of graphene is facile, inexpensive and can easily be scaled up [14]. It has also been reported that graphene/polymer composites exhibit improved thermal, electrical and mechanical properties compared to other nanostructured carbon fillers at similar volume fractions whilst retaining the processability of the polymer, thus allowing the fabrication of complex three-dimensional structures.[15, 16] In addition, there have been many reports indicating the harmful effects of carbon nanotubes both in vitro and in vivo [17, 18], while recent work has shown that not only is graphene a biocompatible material but it can also be beneficial in cell growth.[4, 5]

Most work on composites of biopolymers and graphenic materials has been carried out with non-conducting graphene oxide (GO). [19, 20] More specifically, a number of authors have shown that the addition of GO can improve the mechanical properties of chitosan films significantly [21, 22] and there are some reports on the effects of graphene oxide on the biocompatibility of graphene-chitosan composite films.[10, 23] However, very little work has been done to study the effect of the addition of well dispersed, electrically conductive graphene nanosheets on the chitosan matrix.

Although acetic acid is the most commonly used solubilizing cross-linking acid in the preparation of chitosan and chitosan composite films, it must be utilised with care in biomedical applications as it can cause adverse effects on cell growth. [24] Lactic acid, on the other hand, plays a pivotal role in many biochemical reactions, has been shown to be less cytotoxic than acetic acid and has hydroxyl and a carboxyl functional groups making it an ideal cross-linking agent for chitosan entangled hydrogels for biomedical applications.[24, 25] It has also been shown that the chitosan films made using lactic acid exhibit improved mechanical properties making them promising candidates for fabricating scaffolds for tissue engineering.[26-28]

In this work, we have prepared conducting biocompatible hydrogels using chitosan and lactic acid as the matrix. Graphene was used as a filler to improve the mechanical properties and conductivity of the hydrogels. We have developed a facile preparation method for producing graphene/chitosan composites that can be cast as films or extrusion-printed into 3D scaffolds. Cell studies demonstrated that the composites are biocompatible and show good potential to be used in future tissue engineering studies.

Materials and Methods

Materials

Chitosan powder (medium molecular weight) and P_2O_5 were purchased from Sigma-Aldrich. Graphite powder was obtained from Bay Carbon. Acetic acid, sulphuric acid and 30 % H_2O_2 were purchased from Ajax Finechem. DL-lactic acid (80-85% aqueous solution) was purchased from Alfa Aesar. $K_2S_2O_8$ and $KMnO_4$ were obtained from Chem-supply. Milli-Q water with a resistivity of 18.2 mΩ cm^{-1} was used in all preparations.

Preparation of chemically reduced graphene oxide dispersion

Graphene oxide (GO) was synthesized from natural graphite powder using a modified Hummers' method in two steps using $K_2S_2O_8$, P_2O_5 and H_2SO_4 followed by H_2SO_4, $KMnO_4$ and H_2O_2 to achieve better oxidation of

graphite.[29, 30] The synthesized GO was suspended in water and sonicated for 80 min to create a 0.05 wt% exfoliated GO dispersion. The resulting brown dispersion was mixed with hydrazine and ammonia and was kept at 95°C under stirring for 1 hour. The weight ratio of hydrazine to GO was fixed at 7:10. The resulting aqueous graphene dispersion (CCG) with a graphene concentration of 0.5 mg ml^{-1} was stable for several weeks. [31]

Preparation of chitosan graphene films

In a typical reaction to prepare the composites, chitosan powder was added to an aqueous graphene dispersion to produce a 2 %w/v solution. The graphene concentration in the final composite was altered by varying the concentration of graphene in the initial CCG dispersion. This was followed by slow addition of lactic acid under stirring. After stirring for 1 hour and sonication for 2 hours, a homogenous dispersion was formed. The solution was cast onto a petri dish and dried at 50°C. The excess, unbound lactic acid was removed by washing the samples in several steps with ethanol/phosphate buffered saline (PBS) solutions decreasing the ethanol/PBS ratio stepwise until the films were in PBS alone. The sample was then well washed with deionised water and was dried in vacuum oven at 50°C until no further weight loss was observed. Graphene chitosan composites were labelled as CSG-0, CSG-0.1, CSG-0.5, CSG-1.5 and CSG-3, according to the weight percentage of the graphene content per chitosan, with CSG-0 containing no graphene and CSG-3 containing 3 wt%. In order to determine the effect of the acid on material properties, materials with acetic acid instead of lactic acid were also prepared in a similar fashion and are labelled CSG-(AA).

Characterization

All testing was carried out at least in triplicate and for tests in the dried state the materials used were dried thoroughly and kept in desiccators until analysis. FTIR spectra were measured between 400 and 4000 cm^{-1} on a Shimadzu IRPrestige-21 infrared spectrometer. The spectra of CSG films were obtained using 1 cm x 1 cm films on an ATR attachment, while transmission mode in KBr was used for chitosan and CCG powders. Raman spectra were recorded on a Jobin Yvon Horiba HR800 Raman microscope using a 632 nm laser line and a 300-line grating. Scanning electron microscopy (SEM) images were taken with a field-emission SEM instrument (JEOL JSM-6490LV). Samples were frozen in liquid nitrogen, fractured and sputter-coated (EDWARDS Auto 306) with a thin layer of gold (≈12 nm thickness). X-ray powder diffraction (XRD) experiments were conducted using GBC MMA diffraction equipment (GBC Scientific Equipment Pty Ltd, Australia) equipped with Cu-κα radiation on CSG-0, CSG-0.5 and CSG-1.5 films (1.5 cm × 1.5 cm) as well as on chitosan powder. Thermal gravimetric analysis (TGA) was performed using a TA Instruments TGA Q500 on 10 mg of CSG-0 and CSG-3 films as well as on CCG and chitosan powder and lactic acid (that is liquid) with a heating rate of $5^{o}C\ min^{-1}$ under a nitrogen atmosphere. All sonication was done using a Branson Digital Sonicator (S450D, 500 W, 40 % amplitude). The mechanical properties of all CSG samples were tested using an Instron 5566 Universal Testing Machine (USA) with TRAPEZIUMX software. To prepare samples for mechanical property tests, the samples were cut into strips with a width of 3 mm and a length of 20 mm. The tensile properties of the samples were measured at a constant rate of 5 mm min^{-1}. The Young's modulus was calculated from the slope of the initial part of the curve, where the relationship between

stress and strain is linear and the mean and standard deviation of tensile strength, elongation at break and Young's modulus was reported for n=5 samples. The electrical conductivity of the composite films was measured using a four-point probe resistivity measurement system (JG 293015 Jandel) at ambient temperature. All the conductivity values are the average of five consecutive measurements. Freeze-dried samples were prepared using a ALPHA 2- 4 LD (Martin Christ, Germany) freeze dryer. In order to measure the swelling properties, the samples were first fully dried in vacuum oven at 50°C until no further weight loss was observed and then a known weight of sample was measured by immersing the samples in DI water and weighing them at different time intervals (30s, 1min, 2min, 3min, 4min, 5min, 10min, 15min, 30min, 1hr, 5hrs, 24hrs and 48hrs). The wet weight of the composite was determined by removing adsorbed water from the surface, then weighing the wet composite immediately on an electronic balance. The percentage swelling of the composite in the water were then calculated from the formula:

$$E_{sr} = [(W_s - W_d)/ W_d] \times 100 \quad (1)$$

where E_{sr} is the percent swelling of the sample, W_s denotes the weight of the sample in the swollen state and W_d is the initial weight of the sample.

Fabrication of Scaffolds

Extrusion printing of various CSG blends was conducted on aqueous dispersions at a concentration of 2 wt% chitosan in water using a custom modified computer numerical control (CNC) milling machine (Sherline Products, CA). The system was equipped with a three-axis positioning platform and controlled by the software interface (EMC2), supplied by the manufacturer. An attachment for syringe deposition was built and connected to a controllable gas flow regulator (1-100 psi). The regulator was controlled using a Pololu SciLabs USB-to-serial microcontroller and with an in-house software interface. Thirty layers of each CSG dispersion were printed at 0˚/90˚ orientation onto a glass slide positioned in a precipitating bath of isopropyl alcohol. Scaffolds were fabricated from a 200 µm diameter nozzle fitted to a disposable syringe (Nordson EFD) at a feed rate of 150 mm min^{-1} and with a strand spacing of 0.6 mm giving a final size of 1.5 × 1.5 cm.

Growth of mammalian cells in diluted CSG dispersion

L-929 cells (mouse fibroblast cells) were grown to 80 % confluence in to DMEM+5 % foetal bovine serum before the cells were trypsinised and seeded into 96-well plates at 3200 cells cm^{-2} and allowed to settle for 24 hours, with four wells seeded for each sample. After this period, the media was changed to DMEM+5 % foetal bovine serum with 5 % (v/v) CSG dispersions (giving a final concentration in solution of 0.1 % w/v chitosan and 0.02 % w/v graphene). The cells were cultured for a further 5 days, and imaged by light microscopy before the viability of the cells was analysed by flow cytometry. Briefly, the cell media was removed and the cells exposed to 100 µl 0.025 % trypsin/EDTA for 2 mins before 20 seconds of trituration and addition of 1 µl of 1 mg ml^{-1} propidium iodide, with immediate analysis of cells by flow cytometry (BD Accuri C6 flow cytometer, BD Biosciences). The percentage of live cells and the density of cells were estimated using this method.

Growth of mammalian cells on CSG films and scaffolds

Discs of deacidified CSG films of various graphene contents with a 6 mm diameter were punched under swollen conditions, and the discs were placed into 96-well plates. Cylinders made out of MED610 (Objet,

USA), a biocompatible UV-curable polyacrylic, were used to hold the discs in place and provide a barrier to cell attachment during L-929 seeding at 6000 cells cm^{-2}. The cells were grown for 48 hours, and then underwent live/dead staining (by addition of 1 µM calcein AM (Invitrogen) and 1 µg ml^{-1} propidium iodide (Sigma). Additionally, cells seeded at a higher density (12000 cells cm^{-2}) were fixed after 24 hours with 4 % paraformaldehyde and stained with Alexa488-phalloidin (Invitrogen) to image the cytoskeleton and observe the migration of cells under the MED610 barriers. For cell culture on scaffolds, L-929 cells were prepared at $1E^6$ cells ml^{-1} and 300 µl of this solution was used to seed each 1.5 × 1.5 cm CSG-0.5 scaffold, after scaffolds were deacidified using the procedure described for films. Cells were cultured for 24 hours before fixation with 4 % paraformaldehyde and staining with Alexa488-phalloidin (Invitrogen) and 4',6-diamidino-2-phenylindole (DAPI) (Invitrogen). Confocal microscopy was performed using a Leica SP5 confocal microscope, and image processing was performed using Image J (Research Services Branch, National Institute of Mental Health).

Results and Discussion

Chitosan is a natural material that, due to its biocompatibility, can be used in a wide range of biomedical applications.[32-34] However, its lack of processibility is a major drawback; chitosan is insoluble in pure water or organic solvents and an acidic medium is required to make a processable chitosan solution. The solubilization of chitosan in organic acids results in entangled hydrogels formed from weak hydrogen bonding with the acid.[35] The acid type and chitosan concentration can play an important role in determining the properties of the resultant chitosan film.[36, 37] Choosing the correct acid type and chitosan concentration becomes more crucial when producing composites with chitosan and filler, as the acid can have a determining effect on the quality of the resulting composites.

Graphene/chitosan composite (CSG) films containing up to 3 wt% reduced graphene oxide were easily prepared by casting a homogeneous dispersion of the appropriate amount of lactic acid with an aqueous mixture of the graphene and chitosan. It was important to find the optimum chitosan/lactic acid ratio as it has a direct effect on the homogeneity of the solution and subsequently the quality of the film. In this case, the optimum chitosan:lactic acid ratio was found to be 1:2 w/w (Table S1). The CSG films were thoroughly washed and dried and characterised by thermogravimetric analysis, scanning electron microscopy, infrared and Raman spectroscopy, X-ray diffraction analysis and conductivity measurements, prior to mechanical testing.

Scanning Electron Microscopy

Scanning electron microscopy (SEM) was used to determine the quality of the dispersion of reduced graphene oxide nanosheets in the polymer matrix. Fig. 1 shows SEM images of chitosan films with different graphene loadings.

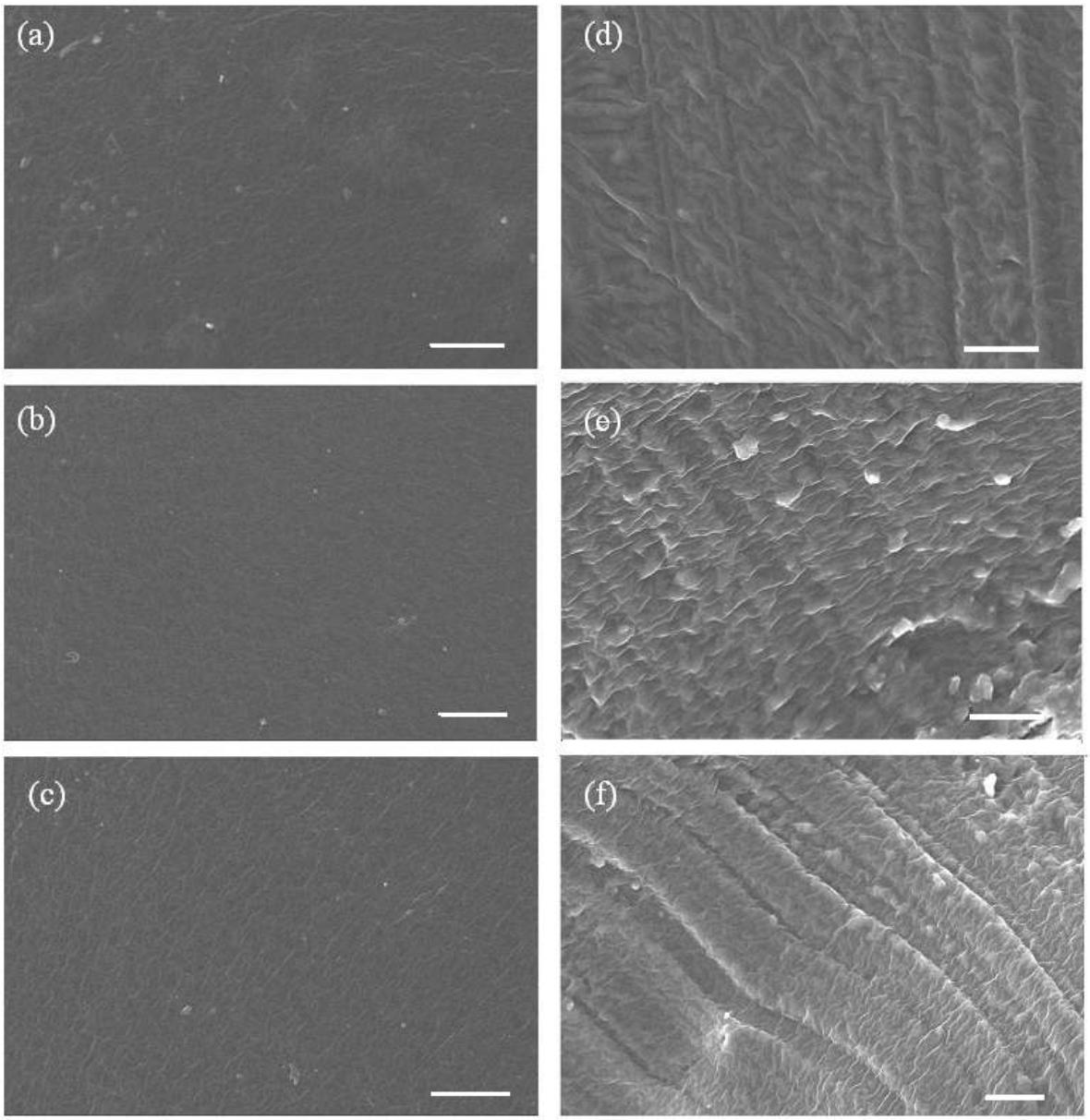

Fig. 1 SEM images of the surfaces (a-c) and cross sections (d-f) of CSG-0 (a,d), CSG-1.5 (b,e) and CSG-3 (c,f) films. The scale bar represents 200 μm.

The addition of graphene causes no obvious induced surface porosity in the images of the film surfaces and there is no evidence of agglomeration indicating good dispersion of graphene sheets in the chitosan matrix without observable aggregation.

Comparing the cross-sectional images, the inner structure of CSG-1.5 and CSG-3 appears much dense and stratified than that of CSG-0 which, as all samples were prepared similarly, is most likely due to differing compositions and interfaces. This is indicative of a strong interaction between chitosan and graphene. This strong interaction can be observed empirically in the enhancement of the tensile strength by increasing the graphene content as observed in mechanical properties test.

Material Composition

Thermal studies showed that following the removal of unbound excess lactic acid using a multi-step washing

procedure, the CSG composites consisted of a complex hydrogen-bonded lactic acid/graphene/chitosan material with increased thermal stability (Fig. S1). Infra-red spectroscopy was used to probe and clarify the interactions between graphene and the chitosan/lactic acid matrix (Fig. 2a). Two absorbance bands at 1658 and 1573 cm^{-1} correspond to the C=O stretching vibration and the N–H bending of the NH_2 groups of chitosan, respectively. The peaks at around 3400 cm^{-1} correspond to the N–H stretching vibration of the NH_2 groups. The absorption peaks from 1037 to 1153 cm^{-1} are attributed to primary and secondary alcohol groups, as well as the chitosan primary amine functionality. The peak at 1720 cm^{-1} is assigned to the carboxyl groups from reduced graphene oxide and the bands around 2800-3000 cm^{-1} correspond to characteristic C–H stretches. The spectrum of CCG appears as a straight line due to elimination of most of the defect oxygen functional groups.

The bands corresponding to the C=O characteristic stretching band of the amide group (1658 cm^{-1}), N–H bending of $-NH_2$ (1573 cm^{-1}) and N–H stretching vibration of the amino groups (3464 cm^{-1}) in chitosan shift to a lower wavenumber in composite films, indicating likely hydrogen bonding interactions between chitosan and lactic acid and reduced graphene oxide.

Raman spectra were collected on chitosan films and the CSG composites between 400 and 2500 cm^{-1} (Fig. 2b). In chitosan, the peak at 898 cm^{-1} is attributed to NH_2 wagging. The multiple peaks around 1099 cm^{-1} can be attributed to ether bonds and the stretching of glycosidic bonds and the band at 1377 cm^{-1} is associated with methyl group bends.[38] In the spectra of the graphene composites, there are two significant peaks at 1328 and 1598 cm^{-1} corresponding to the D and G bands of the incorporated graphene sheets. On increasing graphene content, the peaks due to chitosan films are less visible as the intensity of the characteristic D and G bands of graphene are greater than that of the chitosan bands. In samples with highest graphene content, only the D and G graphene bands are visible. The D and G bands show no shift and the I_D/I_G ratio is virtually unchanged from the pristine graphene to the graphene composites, indicating little or no change in the sp^2 nature and size of the graphene nanosheets. [39, 40].

(a)

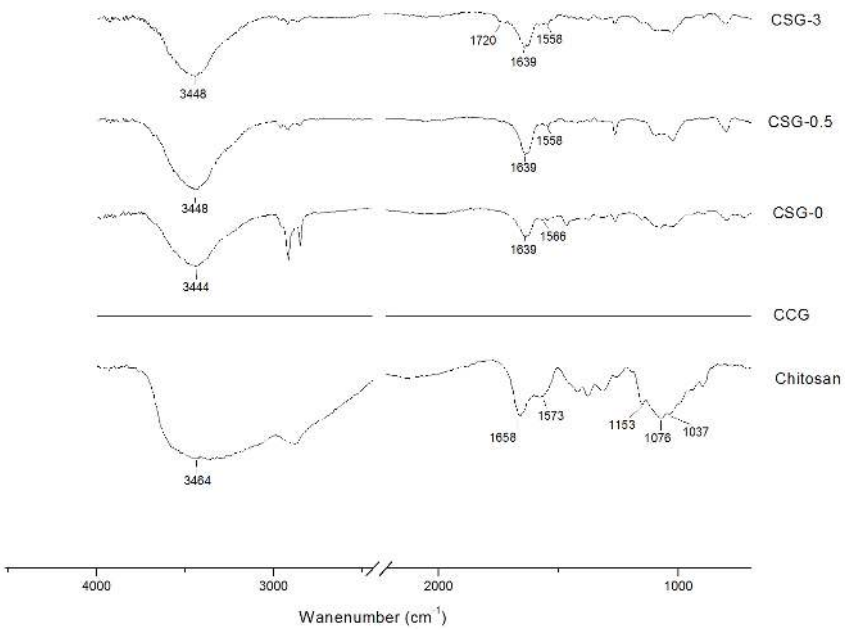

(b)

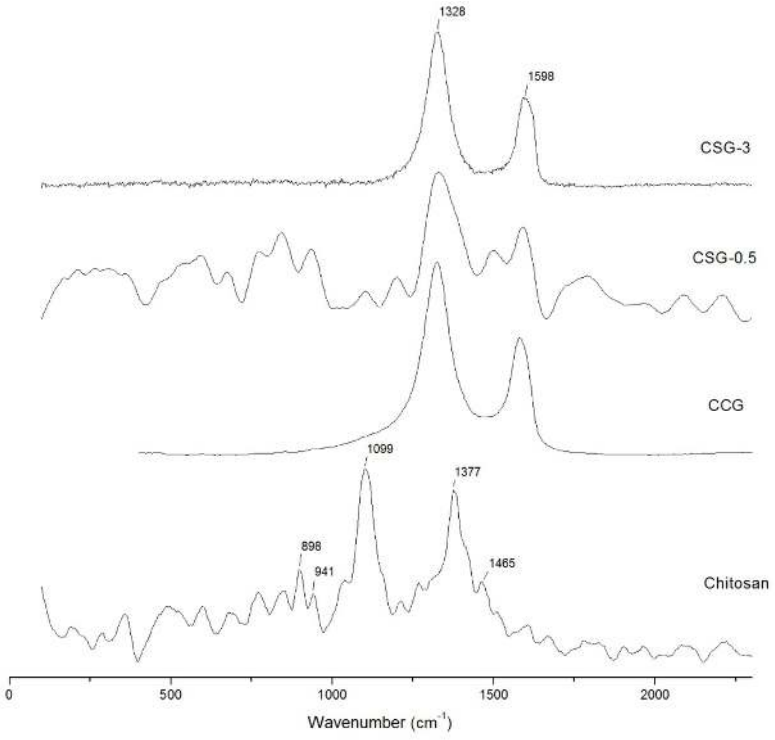

Fig. 2 (a) FTIR spectra of chitosan, CCG and graphene/chitosan composites containing 0 wt% graphene (CSG-0), 0.5 wt% graphene (CSG-0.5) and 3 wt% graphene (CSG-3) and (b) Raman spectra of pristine chitosan, CCG and graphene/chitosan composites containing 0.5 wt% graphene (CSG-0.5) and 3 wt% graphene (CSG-3).

X-ray Diffraction

The XRD patterns of the films are shown in Fig. 3. Pure chitosan shows two major peaks at 2θ = 10.7°, corresponding to the hydrated crystalline structure, and 2θ = 21.2° corresponding to the amorphous state of chitosan.[41, 42] The reduction in diffraction intensity at 2θ = 10.7° and the broadening of the amorphous peak on the addition of lactic acid and graphene implies a decrease in

the degree of crystallinity of the chitosan in the composites. It is likely that the chitosan forms an amorphous network in an entangled hydrogel preventing graphene nanosheets from functioning as multiple nucleating centres in the crystallisation of the polymer as has been seen previously in graphene/polymer composites.[15]

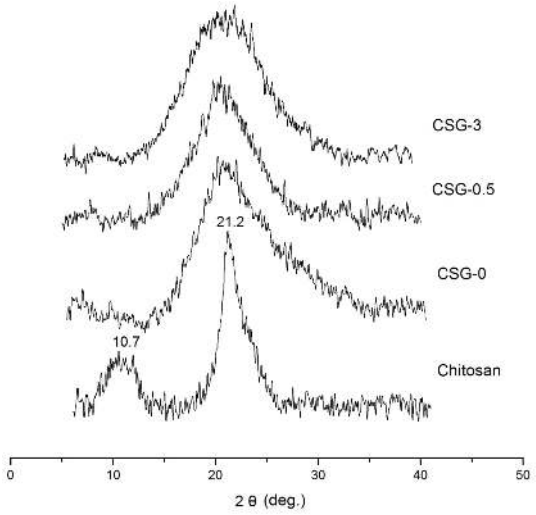

Fig. 3 XRD patterns of chitosan and chitosan/lactic acid composite films containing no graphene (CSG-0), 0.5 wt% graphene (CSG-0.5) and 3 wt% graphene (CSG-3).

Conductivity

Chitosan is generally an insulating material in its pristine state (conductivity less than $1E^{-8}$ S m^{-1} [43]) and previous work on graphene chitosan blends have used insulating GO and have not affected the conductivity. [10, 21, 44, 45] However, as expected, the conductivity of the composites increases with increasing addition of conducting chemically converted graphene content (Fig. 4). In composite films prepared using lactic acid, addition of just 3 wt% graphene improves the conductivity to $1.33E^{-1}$ S m^{-1}. There is also a very low percolation threshold in the dry state with addition of less 0.1 wt% graphene resulting in conductivities that are orders of magnitude higher than the pristine polymer.

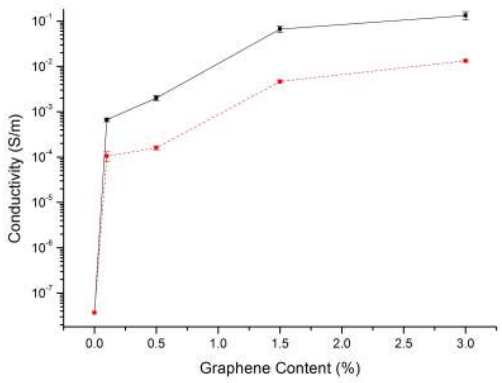

Fig. 4 Conductivity measurements of CSG composites produced using (■) lactic acid and (●) acetic acid. The conductivity of pristine chitosan is taken to be approximately $1E^{-8}$.[43]

Similar films produced using acetic acid instead of lactic acid show conductivity consistently one order of magnitude less than those made with lactic acid. The greater conductivity due to the presence of lactic acid is probably due to the improved dispersion of graphene throughout the polymer matrix, most likely owing to the formation of a greater number of hydrogen bonds among hydroxyl and carboxylic groups of the composite components.

Swelling Studies

The swelling characteristics of the chitosan composites were determined by swelling the composite in DI water at room temperature with the swelling %, E_{sr}, calculated using Equation 1 (see Materials and Methods section). Lactic acid/chitosan (CSG-0) swells up to 400 % in the first 10 min and up to 500 % in DI water within 6 hours. As is clearly apparent in Fig. 5, the swelling of the CSG composites could be controlled by the addition of graphene with swelling decreasing with increasing graphene content, presumably due to the interaction between the polymer matrix and the hydrophobic graphene nanosheets. Acetic acid/chitosan films (CSG-AA) on the other hand, showed significantly less swelling

than that achieved by lactic acid/chitosan matrices, with the maximum swelling found to be just 148 %.

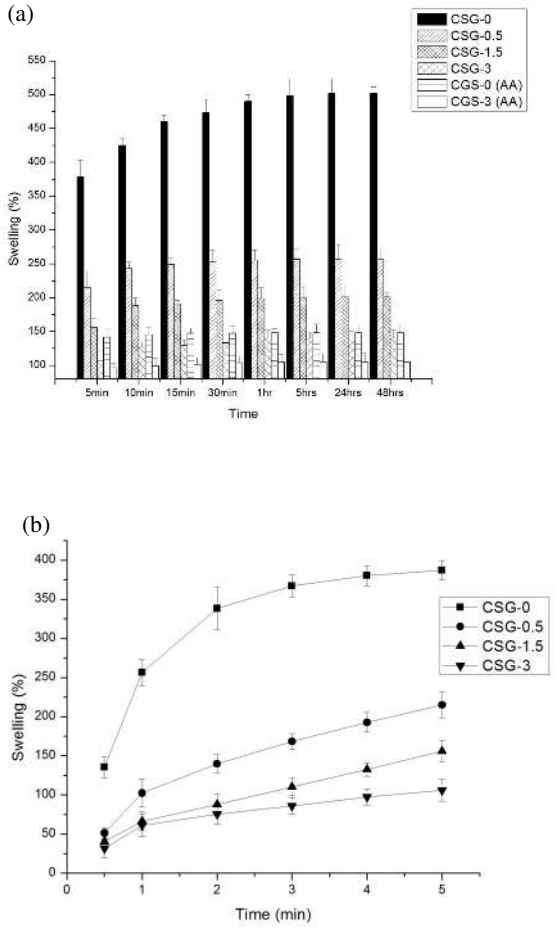

Fig. 5 (a) Swelling characteristics of the lactic acid/chitosan composites (CSG) and acetic acid/chitosan composites (CSG (AA)) in deionised water over 48 hours and (b) the CSG composite swelling rates in the first five minutes.

Mechanical properties

Typical stress–strain curves for chitosan films with different graphene loadings are shown in Fig. 6. The tensile strength and modulus of the composites in the dry state significantly increase with increasing graphene content with only a small decrease in elongation on break (Fig. 6a). On incorporation of only 0.5 wt% graphene, the tensile strength is improved by more than 58 %, whereas the addition of 3 wt% graphene improved the tensile strength by more than 223 % and the Young's modulus by more than 135 % (Table 1). The improvement in tensile strength and modulus of the composites indicates good dispersion of graphene sheets in the composite matrix and the strong interaction between graphene and the other components of the composite. As expected, the tensile strength of the samples is reduced in their swollen state as water molecules interact strongly with the hydroxyl groups of chitosan, resulting in swelling and weakening of intermolecular H-bonds (Fig. 6b). As such, the tensile strength of the swollen chitosan lactic acid film is approximately 230 kPa. Addition of graphene increased the tensile strength to more than 372 kPa even in the swollen state partly as a result of the reduced swelling degree (Table 1). These increases of more than 200% in tensile strength and 130% in modulus compare well with previous studies and even exceed the improvements in mechanical properties shown on the addition of non-conducting GO to chitosan.[21, 44, 45]

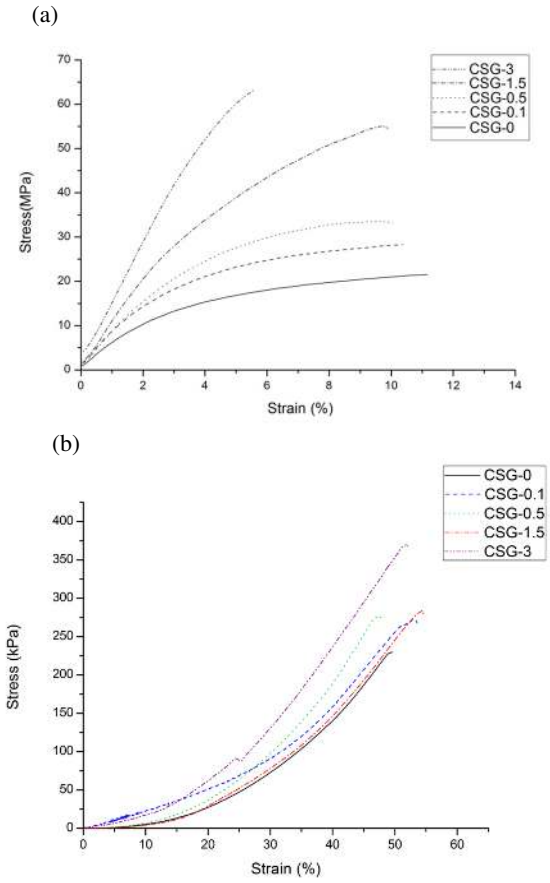

Fig. 6 Stress-strain curves of CSG samples in (a) the dry state and (b) the swollen wet state

Table 1. Mechanical properties of chitosan composites with different graphene contents in the wet and dry state.

Sample	Dry State			Wet State	
	Tensile strength [MPa]	Elongation at break [%]	Young's Modulus [MPa]	Tensile strength [kPa]	Elongation at break [%]
CSG-0	21.1±1.5	11.2±0.3	577.5±25	229.7±4	50.8±6
CSG-0.1	28.5±2.3	10.3±0.5	733±30	272±10.6	53.6±4
CSG-0.5	33.5±1.3	10±0.6	786.6±48	275.7±7	48±4
CSG-1.5	55.75±1.8	9.8±0.9	986.9±90	283.5±11	54.8±6
CSG-3	68.3±1.3	5.6±0.8	1358.6±75	372.2±11	51.61±6

On the other hand, swollen samples show much better elongation at break compared to dried samples (Fig. 6b). Elongation at break of the swollen CSG-0 is around 50 %, more than four times higher than the dried material, and swollen CSG-3 is almost 9 times higher than dried films.

Scaffold Printing

Three-dimensional fabrication is an important aspect of tissue engineering as developing scaffolds with controlled dimensions is vital for implantation. Cells are cultured on scaffolds to grow and re-implanted into patients to regenerate damaged tissues. During the formation of the new tissue, the scaffold biodegrades and can be absorbed or discharged by the body. Three dimensional structures can easily be produced by freeze drying the CSG solutions. The resulting highly porous, conducting materials exhibit very high surface area and extremely low density (Fig. S2). However, for tissue engineering applications, control over the morphology, dimensions and shape of the final scaffold are crucial so a more controlled method of fabrication is required. Due to the low percolation threshold, a minimal amount of graphene is required to produce these composites so the processability of the polymer is retained and three-dimensional CSG scaffolds can be extrusion printed.

Graphene/chitosan composites were successfully extrusion printed into fibres of varying diameters and scaffolds of 1.5 × 1.5 cm in dimension and a pore size of 500 × 500 µm. Fig. 7a,b shows a scaffold containing 0.5 wt% graphene content printed to thirty layers and Fig. 7c

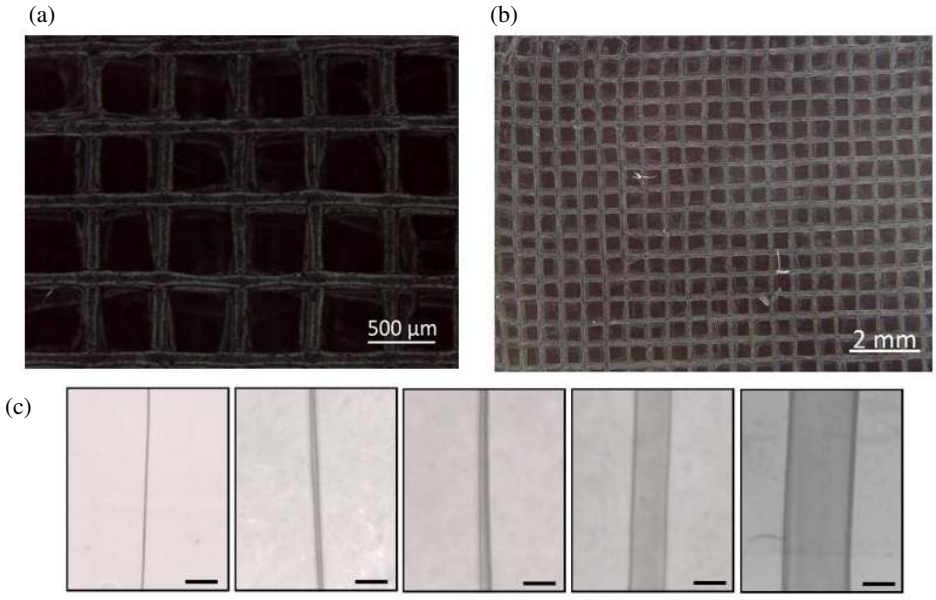

Fig. 7 Optical images of 0.5 wt% graphene/chitosan (CSG-0.5) scaffolds fabricated by extrusion printing at (a) high and (b) low resolution, and (c) 0.5 wt% graphene/chitosan (CSG-0.5) fibres extrusion printed with diameters varying between 50 µm to 1 mm (the scale bars represent 500 µm).

represents printed fibres with diameters varying between 50 µm to 1 mm. The dimensions of the scaffold, including the number of layers and the pore size can be easily varied based on the final application of the product.

Biocompatibility

Growth of mammalian cells in diluted CSG dispersions. Before cells were grown on the composite scaffold, healthy fibroblast cells were exposed to graphene/chitosan dispersions. This was done in order to determine any toxic effects of the components of the materials not confined in a solid material, as the toxicity of graphene due to penetration of the cell membrane is likely to be limited in the composite material. Assessing the effect of graphene and chitosan diluted in solution (5 % v/v chitosan/graphene solution into cell culture media and exposed to cells for 5 days) was undertaken using flow cytometry in order to determine any potential effects of the products of degradation from the degradable hydrogels. The density of the cells increased by 10-15 times over the seeding density for all conditions, with final densities and proportions of dead cells of 45 ± 4 E^4 cells cm^{-2} (1.5 % dead cells) for lactic acid CSG dispersions, 37 ± 4 E^4 cells cm^{-2} (0.5 % dead cells) for acetic acid CSG dispersions, and 47 ± 4 E^4 cells cm^{-2} (3.5 % dead cells) for the untreated tissue culture controls (Fig. S3a and b). Importantly, the side scatter, which gives a measure of the granularity of cells in flow cytometry, was either unaffected or decreased in graphene-exposed cells compared to control cells, suggesting that graphene had not been taken up by the cells. This is supported by bright field images of the cells growing in the presence of the dispersed graphene (Fig. S3c and d), which demonstrate a normal morphology for fibroblasts, and show no inclusion of dark material in the cytoplasm or any organelle.

Cell culture on CSG films and scaffolds. L-929 cells were grown on a CSG film (CSG-1.5) for 48 hours, before staining with a live-dead cell stain. The images of cells (see Fig. 8a) show that cells adhered well to the film surface and showed a morphology typical of fibroblasts. The proportion of dead cells was very low at less than 0.1 wt%, and the density of the cells was increased over the seeding density. Fig. 8a and Fig. 8b show a comparison of cells grown on the CSG-1.5 film to cells grown on a chitosan-only film under the same culture conditions, demonstrating that the addition of graphene did not affect the attachment or proliferation of cells.

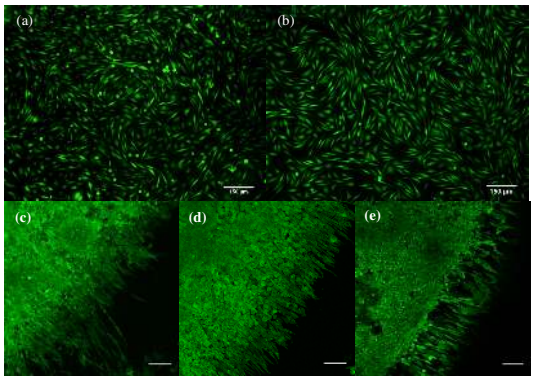

Fig. 8 Fluorescence microscope images of L-929 fibroblast cells growing on a (a) CSG film and (b) tissue culture plastic stained with a live/dead stain. Calcein AM was used to stain metabolically active cells green, and propidium iodide to stain the nuclei of cells with compromised membrane integrity red. Scale bars represent 150 µm. Microscope images in (c), (d) and (e) show fibroblast migration under a barrier over 24 hours on (c) tissue culture plastic, (d) a chitosan film and (e) CSG film. The cytoskeleton of the fixed cells were stained with Alexa-488 phalloidin before confocal microscopy, and the scale bars represent 100 µm.

The migratory capabilities of fibroblast cells seeded at a higher density on chitosan and CSG-1.5 films were also compared to the migration on tissue culture plastic by

providing a barrier to cell attachment (a cylinder of MED610, a UV-curable acrylic placed on top of the culture area), and observing the ingrowth of cells under the barrier. Representative images of fixed cells after 24 hours of growth are shown in Fig. 8c, d and e. The average distance of migration (± one standard deviation) on the three surfaces was 200 ± 100 µm for tissue culture plastic, 180± 30 µm for CSG-0 films and 180± 30 µm on CSG-1.5 films. The higher standard deviation for the control was due to several isolated areas around the culture well where cells had crossed completely across the barrier area (as shown in Fig. 8c), however the main cell migration front was similar in size to those observed on both chitosan and CSG films. The cells were observed to migrate a comparable distance on the CSG films to the tissue culture optimised control surface, indicating that the adhesion and metabolism of the fibroblast cells were not significantly affected by either the graphene or de-acidified chitosan. This demonstrates the acute biocompatibility of the materials, which caused no toxicity or changes in proliferation or migration ability compared to tissue culture controls over 48 hours.

Finally, L-929 fibroblast cells were grown on printed scaffolds as described above. The 30 layer scaffolds were extruded from CSG-0.5, with a fibre diameter of 100 µm and a pore size of 500 µm. Prior to cell culture, scaffolds were de-acidified, and cells were seeded using 0.3 ml cell solution per scaffold containing 1E ^{6} cells ml^{-1} and incubated for 24 hours before fixing and imaging. As shown in Fig. 9, cells adhered to and proliferated on the scaffolds, and cells were observed on the scaffold surface through all 30 layers.

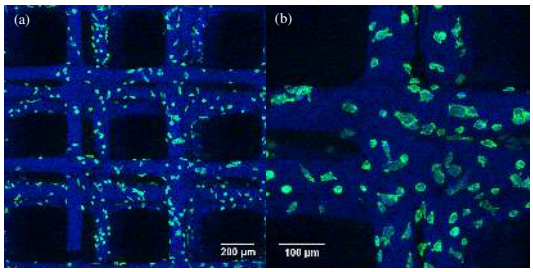

Fig. 9 Z-projected confocal microscope images of L-929 fibroblast cells growing on several layers of an extrusion-printed CSG-05 scaffold. Cell cytoskeletons are stained with Alexa-488-phalloidin (green) and the scaffold and cell nuclei were stained blue with DAPI. The images represent 69 Z-stacks of 2.98 µm (205 µm total Z distance), and the scale bars show 200 µm and 100 µm, respectively.

Conclusion

In this paper, we prepared graphene/chitosan composites through a simple and quick approach using aqueous reduced graphene oxide and lactic acid as a crosslinker. Analysis showed strong hydrogen bond interactions and excellent dispersion of graphene nanosheets in the chitosan/lactic acid matrix. These graphene composites showed large improvements in the conductivity and mechanical properties but retained the processability and swellability of the polymer matrix resulting in a robust, conducting material that could be extrusion-printed into three-dimensional scaffolds. These large improvements at such low graphene contents minimize the risk of accumulation of graphene on degradation and with fibroblast cells exhibiting good proliferation, adherence and viability on the graphene/polymer surfaces suggests that they are excellent candidates for biodegradable materials in tissue engineering cell scaffolds. Compared to previous works that used carbon nanotubes to make hydrogel hybrids, our graphene/chitosan composites show similar or better increases in conductivity and mechanical properties as well as low cost of production, easy dispersibility and most importantly a lack of toxicity.

Acknowledgements

This work has been supported by the Australian Research Council (ARC) under Superscience and Australian Laureate Fellowship funding schemes and the Australian National Fabrication Facility (ANFF). We also acknowledge use of the facilities and the assistance of Mr. Tony Romeo at the UOW Electron Microscopy Centre (EMC).

Notes and References

[a] ARC Centre of Excellence for Electromaterials Science (ACES), Intelligent Polymer Research Institute, AIIM Facility, Innovation Campus, University of Wollongong, NSW 2522, Australia.
[b] Institute for Sports Research, Nanyang Technological University, 50 Nanyang Ave, Singapore 639798, Singapore
[c] School of Mechanical and Aerospace Engineering, Nanyang Technological University, 50 Nanyang Ave, Singapore 639798, Singapore

† Electronic Supplementary Information (ESI) available: The effect of lactic acid on the composite preparation, Thermogravimetric analysis, Freeze drying, Growth of mammalian cells in diluted CSG dispersions. See DOI: 10.1039/b000000x/

1. G. P. Chen, T. Ushida and T. Tateishi, *Macromolecular Bioscience*, 2002, 2, 67-77.
2. M. I. Sabir, X. X. Xu and L. Li, *Journal of Materials Science*, 2009, 44, 5713-5724.
3. S. Jain, A. Sharma and B. Basu, *Biomaterials*, 2013, 34, 9252-9263.
4. S. Y. Park, J. Park, S. H. Sim, M. G. Sung, K. S. Kim, B. H. Hong and S. Hong, *Advanced Materials*, 2011, 23, H263-+.
5. C. Heo, J. Yoo, S. Lee, A. Jo, S. Jung, H. Yoo, Y. H. Lee and M. Suh, *Biomaterials*, 2011, 32, 19-27.
6. M. Rinaudo, *Progress in Polymer Science*, 2006, 31, 603-632.
7. X. F. Shi, J. L. Hudson, P. P. Spicer, J. M. Tour, R. Krishnamoorti and A. G. Mikos, *Biomacromolecules*, 2006, 7, 2237-2242.
8. C. Lau, M. J. Cooney and P. Atanassov, *Langmuir*, 2008, 24, 7004-7010.
9. J. V. Veetil and K. M. Ye, *Biotechnology Progress*, 2009, 25, 709-721.
10. H. Fan, L. Wang, K. Zhao, N. Li, Z. Shi, Z. Ge and Z. Jin, *Biomacromolecules*, 2010, 11, 2345-2351.
11. A. K. Geim and A. H. MacDonald, *Physics Today*, 2007, 60, 35-41.
12. K. P. Loh, Q. L. Bao, P. K. Ang and J. X. Yang, *Journal of Materials Chemistry*, 2010, 20, 2277-2289.
13. C. N. R. Rao, K. Biswas, K. S. Subrahmanyam and A. Govindaraj, *Journal of Materials Chemistry*, 2009, 19, 2457-2469.
14. S. Gambhir, E. Murray, S. Sayyar, G. G. Wallace and D. L. Officer, *Carbon*, 2014, 76, 368-377.
15. S. Sayyar, E. Murray, B. C. Thompson, S. Gambhir, D. L. Officer and G. G. Wallace, *Carbon*, 2013, 52, 296-304.
16. S. Sayyar, R. Cornock, E. Murray, S. Beirne, D. L. Officer and G. G. Wallace, *Materials Science Forum*, 2013, 773 - 774, 496-502.
17. Y. G. Han, J. Xu, Z. G. Li, G. G. Ren and Z. Yang, *Neurotoxicology*, 2012, 33, 1128-1134.
18. J. P. Cheng and S. H. Cheng, *International Journal of Nanomedicine*, 2012, 7, 3731-3739.
19. L. Zhang, Z. P. Wang, C. Xu, Y. Li, J. P. Gao, W. Wang and Y. Liu, *Journal of Materials Chemistry*, 2011, 21, 10399-10406.
20. S. R. Shin, B. Aghaei-Ghareh-Bolagh, T. T. Dang, S. N. Topkaya, X. G. Gao, S. Y. Yang, S. M. Jung, J. H. Oh, M. R. Dokmeci, X. W. Tang and A. Khademhosseini, *Advanced Materials*, 2013, 25, 6385-6391.
21. D. Han, L. Yan, W. Chen and W. Li, *Carbohydrate Polymers*, 2011, 83, 653-658.
22. Y. Pan, T. Wu, H. Bao and L. Li, *Carbohydrate Polymers*, 2011, 83, 1908-1915.
23. X. Wang, H. Bai, Z. Yao, A. Liu and G. Shi, *Journal of Materials Chemistry*, 2010, 20, 9032-9036.
24. S. E. Hismiogullari, A. A. Hismiogullari, F. Sahin, E. T. Oner, S. Yenice and D. Karasartova, *Journal of Animal and Veterinary Advances*, 2008, 7, 681-684.
25. R. A. Auras, L.-T. Lim, S. E. M. Selke and H. Tsuji, *Poly(Lactic Acid): Synthesis, Structures, Properties, Processing, and Applications*, John Wiley & Sons, 2011.
26. K. M. Kim, J. H. Son, S. K. Kim, C. L. Weller and M. A. Hanna, *Journal of Food Science*, 2006, 71, E119-E124.
27. N. Niamsa and Y. Baimark, *American Journal of Food Technology*, 2009, 4, 162-169.
28. Y. Zhong, X. Y. Song and Y. F. Li, *Carbohydrate Polymers*, 2011, 84, 335-342.
29. W. S. Hummers and R. E. Offeman, *Journal of the American Chemical Society*, 1958, 80, 1339-1339.
30. N. I. Kovtyukhova, P. J. Ollivier, B. R. Martin, T. E. Mallouk, S. A. Chizhik, E. V. Buzaneva and A. D. Gorchinskiy, *Chemistry of Materials*, 1999, 11, 771-778.
31. D. Li, M. B. Muller, S. Gilje, R. B. Kaner and G. G. Wallace, *Nat Nanotechnol*, 2008, 3, 101-105.
32. J. K. Francis Suh and H. W. T. Matthew, *Biomaterials*, 2000, 21, 2589-2598.
33. H. Y. Tai, S. H. Chou, L. P. Cheng, H. T. Yu and T. M. Don, *Journal of Biomaterials Science-Polymer Edition*, 2012, 23, 1153-1170.
34. L. Casettari, D. Vllasaliu, J. K. W. Lam, M. Soliman and L. Illum, *Biomaterials*, 2012, 33, 7565-7583.
35. J. Berger, M. Reist, J. M. Mayer, O. Felt, N. A. Peppas and R. Gurny, *European Journal of Pharmaceutics and Biopharmaceutics*, 2004, 57, 19-34.
36. C. A. Kienzlesterzer, D. Rodriguezsanchez and C. K. Rha, *Makromolekulare Chemie-Macromolecular Chemistry and Physics*, 1982, 183, 1353-1359.
37. S. Y. Park, K. S. Marsh and J. W. Rhim, *Journal of Food Science*, 2002, 67, 194-197.
38. C. E. Orrego, N. Salgado, J. S. Valencia, G. I. Giraldo, O. H. Giraldo and C. A. Cardona, *Carbohydrate Polymers*, 2010, 79, 9-16.
39. M. A. Pimenta, G. Dresselhaus, M. S. Dresselhaus, L. G. Cancado, A. Jorio and R. Saito, *Physical Chemistry Chemical Physics*, 2007, 9, 1276-1291.
40. P. Hasin, M. A. Alpuche-Aviles and Y. Wu, *The Journal of Physical Chemistry C*, 2010, 114, 15857-15861.
41. K. Ogawa, S. Hirano, T. Miyanishi, T. Yui and T. Watanabe, *Macromolecules*, 1984, 17, 973-975.
42. J. W. Rhim, S. I. Hong, H. M. Park and P. K. W. Ng, *Journal of Agricultural and Food Chemistry*, 2006, 54, 5814-5822.
43. Y. Wan, K. A. M. Creber, B. Peppley and V. T. Bui, *Macromolecular Chemistry and Physics*, 2003, 204, 850-858.
44. X. Yang, Y. Tu, L. Li, S. Shang and X.-m. Tao, *ACS Applied Materials & Interfaces*, 2010, 2, 1707-1713.
45. L. Shao, X. J. Chang, Y. L. Zhang, Y. F. Huang, Y. H. Yao and Z. H. Guo, *Applied Surface Science*, 2013, 280, 989-992.